Performance Analyses on OFDM-PON in Coherent Detection Schemes

Mingzhi Mao, Rongrong Chen, Caixia Kuang, Rujian Lin
The key Laboratory of Specialty Fiber Optics and Optical Access Networks
Shanghai University
149 Yanchang Road, Shanghai 200072
CHINA
rujianlin@shu.edu.cn http://www.shu.edu.cn

Abstract: - Performance analyses are presented theoretically on OFDM-PON working in IQ modulation-heterodyne detection scheme for downstream and in intensity modulation-homodyne detection scheme for upstream which include the characterization of non-linear distortion in IQ modulator, pilot light multiplexing for optical phase noise cancellation in ONU receiver, heterodyne detection with LO provided by sharing the seed light power to RSOA， downstream system optimization and non-linear optical phase noise cancellation in OLT receiver. Simulation and experiment show that the receiver sensitivity can reach –(21~27) dBm for downstream light at single wavelength carrying 64/16 QAM-modulated OFDM signal in 2GHz band, when LO power is higher than –10 dBm and the receiver sensitivity can reach –20 dBm for upstream light at single wavelength carrying 16 QAM-modulated OFDM signal in1.6 GHz band, when LO power is high than 0 dBm.

Key-Words: - OFDM-PON, IQ modulator, Coherent Detection, Self Homodyne, Heterodyne, MQAM, Non-linear distortion, optical phase noise

1 Introduction

The typical OFDM-PONs considered so far operate in intensity modulation and direct detection scheme, because of its simplicity and cost-effectiveness. But the downstream and upstream links of an OFDM-PON are analog-modulated optical systems. To avoid nonlinear distortion in modulators the optical modulation index for each OFDM sub-channel should be kept below 3 %, hence the receiver sensitivity is poor making the link budget normally less than 15dB, far behind the requirement of NGPON-2. To improve the receiver sensitivity optical IQ modulation and coherent detection could be employed. The classical coherent detection is of intra-dyne (ID) type with a free running laser to provide the local oscillation (LO) for O-E conversion of the received optical signal in a quasi-homodyne style. After detection a digital signal processing (DSP) unit should be employed to perform fiber CD compensation, polarization de-multiplexing, carrier frequency offset and optical phase noise estimation, channel equalization and symbol estimation (CPE). The expense of laser and the complexity of DSP are the major reasons that people exclude the application of coherent detection to ONU, which is cost sensitive.

If a pilot-carrier, generated from the same light source as the signal carrier, is polarization-multiplexed with the signal carrier and transmitted together, then the same frequency and phase of the carriers are kept at homodyne receiver, allowing easy recovery of stable constellation and real-time measurement of bit-error rate (BER). Moreover, the phase noise of light source is cancelled at receiver, therefore the signal source and the local source do not need very narrow line-width as required by intra-dyne detection [1-3]. Because a local laser is avoided, ONU cost can be reduced. However the receiver sensitivity and link budget problem are still in doubt, because the LO optical power is taken from a polarization-de-multiplexer which is in the same order of magnitude as signal light.

From these viewpoints, a research work has been carried out on the downstream path of a reflective OFDM-PON, where the seed light to the colorless RSOA is partially picked up as the LO for heterodyne detection and on the upstream path where self-homodyne scheme is used. After a brief description of system configuration, especially the principle of linear optical phase noise cancellation by pilot-carrier multiplexing, an analysis on receiver sensitivity will be presented including nonlinear distortion in IQ optical modulator, SNR and EVM in receiver output. The optical modulation index will be optimized and the BER performance will be shown experimentally. At last, the principle of nonlinear optical phase cancellation in upstream homodyne receiver is described and demonstrated by simulation.

2 Configuration of OFDM-PON

Based on IQ optical modulation and heterodyne detection an experimental OFDM-PON is configured as shown in Fig.1.

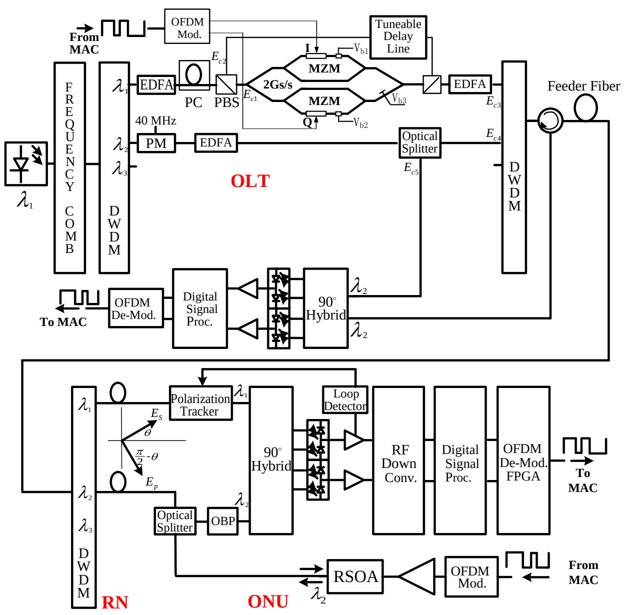

Fig.1 Configuration of OFDM-PON with coherent detection in down- & up-link

In OLT，an optical comb generates 24 light-waves with wavelength interval 0.1nm in C band as shown in Fig.2 (a). Among the comb outputs 10 light-waves are used as downstream signal carriers and other 10 as the seed lights injecting to RSOAs after being transported over the fiber link to construct a reflective PON. Each downstream light-wave carries an OFDM signal in 2 GHz band by IQ optical modulation to a LiN_bO_3 modulator and each upstream light-wave carries an OFDM signal in 1.6 GHz band by intensity modulation to a RSOA. Coherent detection is used both in downstream and upstream reception. The total transmission rates are 100 Gb/s in downstream and 40 Gb/s in upstream respectively by means of the adaptive bit allocation to the OFDM sub-carriers.

For the downstream reception, ONU utilizes a special heterodyne detection scheme with the LO taken from a part of seed light to RSOA, so as to avoid a free running LO laser and keep the coherence of LO to the signal light. In such a way a pure and stable electric carrier at an intermediate frequency (IF) of 12.5 GHz is generated with an associated OFDM sub-band as shown in Fig.2 (b). To reduce the DSP burden in optical phase noise estimation, a pilot light at the same wavelength is polarization-multiplexed with the signal light via two polarized beam splitters in OLT, then the optical phase noise cancellation takes place in the procedures of coherent mixing and RF down-conversion in ONU under the condition of equal time delay between the signal light path and the pilot light path. Therefore a tuneable delay line is inserted in the pilot light path. To make the LO power as strong as possible, a SBS compression method is exploited in OLT by phase modulation on the seed light with an out-of band sinusoidal signal. To reduce the ASE noise effect to SNR degradation a narrow optical band-pass filter (OBP) is installed in front of the LO entrance point of coherent receiver.

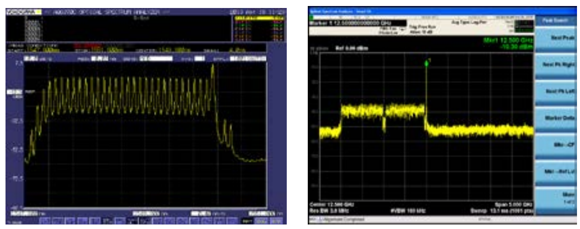

(a) Optical comb (b) Receiver output

Fig.2 Downstream signals

For the upstream reception, a self-homodyne detection scheme is performed in OLT with non-linear optical phase noise cancellation [4].

3 Non-linear Distortion in IQ Optical Modulator

3.1 Transfer Function of IQ modulator

The configuration of IQ modulator composed of two LiN_bO_3 MZMs is shown in Fig.3.

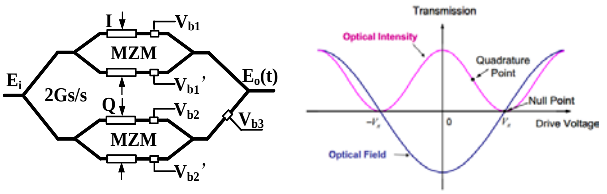

Fig.3 IQ modulator and E-O transfer behaviour

Biased appropriately, the complex envelop of electric field output from the modulator is

$$E_o(t) = -\frac{1}{2}E_i[\sin(\frac{\pi}{2V_\pi}x(t)) - \mathrm{j}\sin(\frac{\pi}{2V_\pi}y(t))] \quad (1)$$

$$x(t) = \sum_k A_k \cos(2\pi k f_s t + \theta_k) \quad y(t) = \sum_k A_k \sin(2\pi k f_s t + \theta_k)$$

where E_i is the amplitude of input electric field; f_s is the frequency of modulation symbol; A_k, θ_k are the amplitude and phase of modulation vector.

The amplitude of output electric field is the function of modulating signal voltage, which is called the transfer function of IQ optical modulator:

$$T_I(x) = \frac{1}{2}\sin[\frac{\pi}{2V_\pi}x(t)] \quad (2)$$

$$T_Q(x) = \frac{1}{2}\sin[\frac{\pi}{2V_\pi}y(t)] \quad (3)$$

The E-O transfer characteristics of IQ optical modulator are shown in Fig.3 where the bias voltages for MZMs are $V_{b1} - V_{b1}' = V_{b2} - V_{b2}' = V_\pi$ (operation point at Null), and $V_{b3} = V_\pi / 2$, where V_π is the half-wave voltage of the modulator. The transfer function is sinusoidal with odd symmetry. It causes the third order distortion of modulating signal $x(t)$ and $y(t)$.

3.2 Expression of electric OFDM signal

The OFDM signal can be expressed in the following:

$$v(t) = x(t) + \mathrm{j}\, y(t) = \sum_{k=1}^{N}\sum_{n=-\infty}^{+\infty} A_{k,n} e^{j\theta_{k,n}} g(t - nT_s) e^{j2\pi k f_s t} \quad (4)$$

where $A_{k,n}$, $\theta_{k,n}$ are the amplitude and phase of modulating vector at the n-th symbol period; $g(t)$ is the waveform of baseband symbol; f_s, T_s are the symbol rate and symbol period of data signal respectively; N is the total number of sub-carriers.

The auto-correlation function of signal $v(t)$ is defined as $R_v(t, t+\tau) = \frac{1}{2}\mathrm{E}\{v^*(t)v(t+\tau)\}$ (where E{ } is mathematical expectation operation), which turns to be [7]:

$$R_v(t, t+\tau) = \sum_{k=1}^{N} \mathrm{e}^{\mathrm{j}2\pi k f_s \tau} \sum_{m=-\infty}^{+\infty} \sigma_k^2 g(t - mT_s) g(t + \tau - mT_s) \quad (5)$$

where $\sigma_v^2 = \sum_{k=1}^{N}\sigma_k^2 = \mathrm{E}\{\sum_{k=1}^{N}\frac{1}{2}A_{k,n}^2\}$ is the average power of OFDM signal.

Because $R_v(t, t+\tau)$ is cyclo-stationary with a time period T_s, a time average is taken to obtain

$$\overline{R_v(\tau)} = \frac{1}{T_s}\sum_{k=1}^{N}\sigma_k^2 \mathrm{e}^{\mathrm{j}2\pi k f_s \tau}\phi_{gg}(\tau) \quad (6)$$

where $\phi_{gg}(\tau)$ is the correlation function of $g(t)$ defined as

$$\phi_{gg}(\tau) = \int_{-\infty}^{+\infty} g(t) g(t+\tau) dt \quad (7)$$

whose Fourier transform is $|G(f)|^2$, where $G(f)$ is the Fourier transform of $g(t)$.

The OFDM signal $v(t)$ is a sum of many amplitude- & phase-modulated subcarriers with independent and equal probability distribution. Therefore it always approximates a Gaussian process if $N > 10$, regardless of the form of probability distribution, according to the central limit theorem.

3.3 The Output Field of IQ Modulator and The Output Power of Receiver

Considering the IQ optical modulator as a non-linear converter, as shown in Fig.4, we relate the input and output Gaussian processes by Rice non-linear conversion theorem [6].

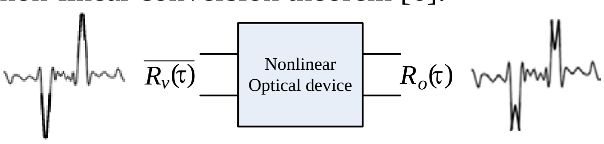

Fig.4 Optical modulator as a non-linear E-O converter

The auto-correlation function of output optical signal from the optical modulator is related to that of input electric OFDM signal as

$$R_o(\tau) = \sum_{k=0}^{\infty}\frac{1}{k!}h_k^2[\frac{\overline{R_v(\tau)}}{\sigma_v^2}]^k$$

$$=\sum_{k=0}^{\infty}\frac{1}{k!}h_k^2\frac{1}{T_s\sigma_v{}^{2k}}\left[\sum_{n=1}^{N}\sigma_n^2 e^{j2\pi nf_s\tau}\phi_{gg}(\tau)\right]^k \quad (8)$$

where $R_o(\tau)$ is the auto-correlation function of output optical OFDM signal; $\overline{R_V(\tau)}$ is the auto-correlation function of input electric OFDM signal; $\sigma_v{}^2$ is the variance of the input electric OFDM signal, i.e. $\sigma_v{}^2=\overline{R_v(0)}$. The zero order term of (8) is the DC component, the first order term is the OFDM signal component and the higher order terms are non-linear distortion components. h_k, the k-th expansion coefficient of the power series, can be expressed as

$$h_k=\frac{1}{\sigma_v}\int_{-\infty}^{+\infty}T(X)H_k(\frac{X}{\sigma_v})\frac{1}{\sqrt{2\pi}}e^{-\frac{X^2}{2\sigma_v{}^2}}dX \quad (9)$$

where $T(X)$ is the transfer function of IQ optical modulator. $H_k(\cdot)$ is the k-th order Hermite polynomial, satisfying the relations:

$H_0(X)=1$, $H_1(X)=X$, $H_n(X)= X H_{n-1}(X)-(n-1) H_{n-2}(X)$ for $n\geq 2$.

Substituting (2) or (3) into (9), the non-linear coefficients of IQ modulator are obtained as

$$h_{2k}=0$$
$$h_{2k+1}=\frac{1}{2}(-1)^k(\frac{\mu}{2})^{2k+1}e^{-\frac{1}{2}(\frac{\mu}{2})^2}\quad k=0,1,2,3\cdots \quad (10)$$

where μ^2, the mean-square optical modulation index of OFDM signal, is defined as

$$\mu^2==(\frac{\pi}{V_\pi})^2\sum_{k=1}^{N}\mathrm{E}\{\frac{1}{2}A_k^2\}=(\frac{\pi}{V_\pi})^2\sigma_v^2 \quad (11)$$

When N sub-carriers are in the same power, we have $\sigma_v^2=N\times\mathrm{E}\{A_1^2/2\}$. This kind of non-linear distortion analysis method has already been published for optical intensity modulators [7]. Here is an extension to optical IQ modulator. It is found from (10) that non-linear coefficient of IQ modulator is much smaller than that of MZM intensity modulator due to the horizontal expansion of modulation transfer function as seen from Fig.3.

Taking the Fourier transform of auto-correlation function (8) and omitting the DC term, we obtain the power spectrum of optical modulator output as

$$S_o(f)=\frac{h_1{}^2}{\sigma_v^2T_s}\sum_{k=0}^{N}\sigma_k^2\left|G(f-kf_s)\right|^2+$$
$$\frac{h_2^2}{2\sigma_v^4T_s^2}\{\sum_{k=0}^{N}\sigma_k^2\left|G(f-kf_s)\right|^2\otimes\sum_{k=0}^{N}\sigma_k^2\left|G(f-kf_s)\right|^2\}+$$
$$\frac{h_3{}^2}{6\sigma_v^6T_s^3}\times\{\sum_{k=0}^{N}\sigma_k^2\left|G(f-kf_s)\right|^2\otimes\sum_{k=0}^{N}\sigma_k^2\left|G(f-kf_s)\right|^2 \quad (12)$$
$$\otimes\sum_{k=0}^{N}\sigma_k^2\left|G(f-kf_s)\right|^2\}+\cdots$$

where the first term represents the OFDM signal; the second term represents the second order distortion products including 2-nd order harmonic and inter-modulation components; the third term represents the third order distortion products including 3-rd order harmonic, carrier compression, cross modulation, intermodulation and triple beat components. Among the second order distortion products, the interference components to sub-channels are 2-nd inter-modulation products falling at frequencies $(j\pm k)f_s$. Among the third order distortion products, the interference components to sub-channels are 3-rd inter-modulation products falling at frequencies $(2j\pm k)f_s$ and triple beat products falling at frequencies $(j\pm k\pm l)f_s$ and dominated by the latter. Gathering all 2-nd order inter-modulation products falling at the frequency nf_s, (n=1,2,…N), and counting the number of products as C_{2n}, also gathering all triple beat products falling at the frequency nf_s, (n=1,2,…N), and counting the number of products as C_{3n}, we obtain the OFDM signal power P_{1n}, the average composite 2-nd order inter-modulation power P_{2n} and the average triple beat power P_{3n} in a symbol period as

$$P_{1n}=K_p\frac{h_1{}^2\sigma_n^2}{\sigma_v^2T_s}\int_{-f_s}^{f_s}\left|G(f)\right|^2df \quad (13)$$

$$P_{2n}=K_p\frac{C_{2n}h_2{}^2\sigma_n^4}{2\sigma_v^4T_s{}^2}\int_{-f_s}^{f_s}[\left|G(f)\right|^2\otimes\left|G(f)\right|^2]df \quad (14)$$

$$P_{3n}=K_p\frac{C_{3n}h_3{}^2\sigma_n^6}{4\sigma_v^6T_s{}^3}\int_{-f_s}^{f_s}[\left|G(f)\right|^2\otimes\left|G(f)\right|^2\otimes\left|G(f)\right|^2]df \quad (15)$$

where $\otimes$ represents the convolution product operation. The optical power output from the modulator and transmitted over the fiber produces the photo-current at the coherent receiver with amplitude equal to the product of $R\sqrt{L}E_iE_L/2$ and the transfer function of optical modulator, where R is the responsivity of photodiode; L is the link loss; $\sqrt{L}E_i=E_s$ is the electric field of received signal light and E_L is the electric field of LO light. Therefore the proportional coefficient of receiver output power is $K_p = R^2 P_S P_L R_L / 2$, where P_S is the optical power of received signal light; P_L is the optical power of LO light; R_L is the load resistance.

If the baseband waveform $g(t)$ is rectangular, its amplitude spectrum is shown in Fig.5(a). The power spectrum of $\phi_{gg}^3(\tau)$ is shown in Fig.5 (b). The related expressions are:

$$g(t)=\begin{cases}1 & |t|\le T_s/2\\ 0 & |t|>T_s/2\end{cases} \tag{16}$$

$$\phi_{gg}(\tau)=\begin{cases}T_s-|\tau| & |\tau|\le T_s\\ 0 & |\tau|>T_s\end{cases} \tag{17}$$

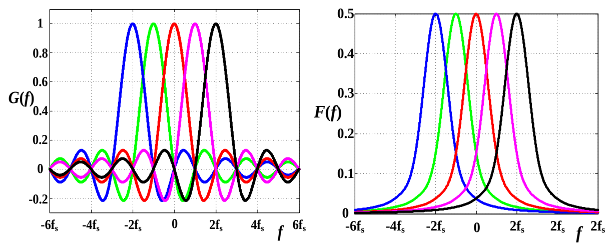

(a) G(f) (b) F(f)

Fig.5 Signal spectrum

$$|G(f)|^2 = T_s^2 \frac{\sin^2(\pi T_s f)}{(\pi T_s f)^2} \tag{18}$$

$$F(f)=|G(f)|^2\otimes|G(f)|^2\otimes|G(f)|^2=\frac{6T_s^2}{(2\pi f)^2}[1-\frac{\sin^2(\pi T_s f)}{(\pi T_s f)^2}] \tag{19}$$

Substituting (18) for $|G(f)|^2$ in (13)~(15) gives

$$P_{1n}=\frac{1}{2}R^2P_SP_LR_L\times 0.9\times h_1^2\frac{\sigma_n^2}{\sigma_v^2} \tag{20}$$

$$P_{2n}=\frac{1}{2}R^2P_SP_LR_L\frac{1}{2}C_{2n}\times 0.8\times h_2^2\frac{\sigma_n^4}{\sigma_v^4} \tag{21}$$

$$P_{3n}=\frac{1}{2}R^2P_SP_LR_L\frac{1}{4}C_{3n}\times 0.7\times h_3^2\frac{\sigma_n^6}{\sigma_v^6} \tag{22}$$

For IQ optical modulator, $h_1=(\mu/4)\mathrm{e}^{-\frac{1}{8}\mu^2}$, $h_2=0$, $h_3=-(\mu^3/16)\mathrm{e}^{-\frac{1}{8}\mu^2}$.

The composite triple beat is defined as:

$$\mathrm{CTB}_n=\frac{P_{3n}}{P_{1n}}=\frac{7C_{3n}}{576N^2}\mu^4 \tag{23}$$

The composite triple beat product number C_{3n} are related to the sub-carrier number N, and distributed along the sub-carrier frequency f_n. For the continuously located N sub-carriers, the maximum C_{3n} occurs at the middle of frequency band where $C_{3n,\max}\approx(N-n)(n-1)/2+N^2/4$, as shown in Fig.6. For example, if the effective number of sub-carriers equals 60 in total 64 sub-carriers, an exhausting computation shows that C_{3n} =1305. A correctly biased IQ optical modulator does not have 2-nd order inter-modulation products and a good RF driving amplifier only has some small inter-modulation products with $C_{2n}\ll C_{3n}$, one should majorly concern about the triple beat distortion when optimizing an OFDM transmission system based on IQ optical modulator.

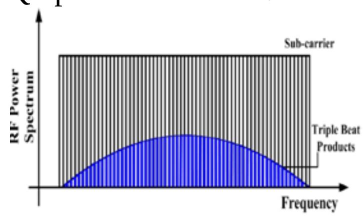

Fig.6 The frequency distribution of the composite triple beat number C_{3n}

4 The Output of Heterodyne Receiver

The typical heterodyne detection receiver with polarization diversity is shown in Fig.7.

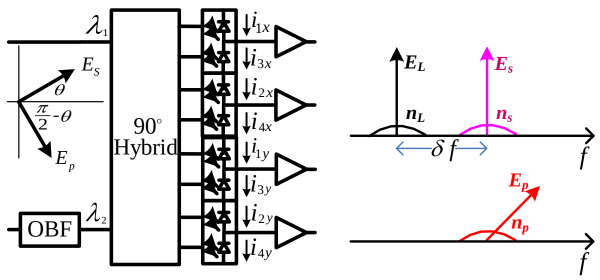

Fig.7 Heterodyne receiver

At TM polarization direction the photo-currents of two pairs of balanced photo-diode are expressed as

$$i_{1x}(t)-i_{3x}(t)\propto$$
$$-R\sqrt{\frac{\alpha}{2}}\sqrt{P_SP_L}\beta\sum_{n=2}^{N}A_n(t)\sin[2\pi(\delta f-nf)t-\phi_n(t)-\phi_c(t)+\phi_c(t-\tau_2)]$$
$$+R\sqrt{\frac{1-\alpha}{2}}\sqrt{P_PP_L}\cos[2\pi\delta f(t)-\phi_c(t)+\phi_c(t-\tau_2)]$$

$$i_{2x}(t)-i_{4x}(t)\propto$$
$$-R\sqrt{\frac{\alpha}{2}}\sqrt{P_S P_L}\beta\sum_{n=2}^{N}A_n(t)\cos[2\pi(\delta f-nf_s)t-\phi_n(t)-\phi_c(t)+\phi_c(t-\tau_2)]$$
$$-R\sqrt{\frac{1-\alpha}{2}}\sqrt{P_P P_L}\sin[2\pi\delta ft-\phi_c(t)+\phi_c(t-\tau_2)]$$

and at TE polarization direction the photo-currents of two pairs of balanced photo-diode are expressed as

$$i_{1y}(t)-i_{3y}(t)\propto$$
$$-R\sqrt{\frac{1-\alpha}{2}}\sqrt{P_s P_L}\beta\sum_{n=2}^{N}A_n(t)\sin[2\pi(\delta f-nf_s)t-\phi_n(t)-\phi_c(t)+\phi_c(t-\tau_2)]$$
$$+R\sqrt{\frac{\alpha}{2}}\sqrt{P_P P_L}\cos[2\pi\delta ft-\phi_c(t)+\phi_c(t-\tau_2)]$$
$$i_{2y}(t)-i_{4y}(t)\propto$$
$$-R\sqrt{\frac{1-\alpha}{2}}\sqrt{P_S P_L}\beta\sum_{n=2}^{N}A_n(t)\cos[2\pi(\delta f-nf_s)t-\phi_n(t)-\phi_c(t)+\phi_c(t-\tau_2)]$$
$$-R\sqrt{\frac{\alpha}{2}}\sqrt{P_P P_L}\sin[2\pi\delta ft-\phi_c(t)+\phi_c(t-\tau_2)]$$

where δf =12.5GHz is the frequency difference between LO light and signal light. $\phi_c(t)$ is the random phase of signal light and pilot light. $\phi_c(t)-\phi_c(t-\tau_2)$ is the optical phase noise with τ_2, the time delay of LO light field relative to signal light field and pilot light field. The polarization factors are $\alpha=\cos^2\theta,\ 1-\alpha=\sin^2\theta$, with θ, the random polarization angle of signal light. $\beta=\pi/(2V_\pi)$ is the optical phase modulation index.

In above expressions the IF frequency (12.5GHz) carrier comes from beating of pilot light and LO light, while the OFDM signal side-band comes from beating of signal light and LO light. Due to the orthogonal state of polarization between pilot light and signal light, the polarization-induced amplitude fluctuation of 12.5GHz carrier is opposite to that of OFDM signal side-band. In the down-conversion step followed, beating between the 12.5GHz carrier and the OFDM signal side-band will result in a baseband OFDM signal with an amplitude factor $\sqrt{\alpha(1-\alpha)}$, which means that the amplitude fluctuation of baseband signal induced by light polarization variation is reduced, but does not disappear. Conventionally, the polarization variation problem is solved by a diversity process in the following DSP. But in the above heterodyne arrangement, the *x* branch and *y* branch of RF down-converter will present two outputs without any difference, making the polarization diversity technique not feasible.

To obtain a stable system output, a polarization tracker with external feedback control is inserted in the signal light path at receiver input as shown in Fig.1. In this way the coherent receiver is simplified to have two pairs of balanced PIN only and one 2x4 90^{o} hybrid.

Because the same optical phase noise is contained in the 12.5GHz carrier and in the OFDM signal side-band, it can be cancelled out in the down-conversion process ideally, leaving the actual residual optical phase noise to be estimated and wiped out in DSP. This method helps to simplify the DSP and is a major advantage of the system presented in Fig.1.

5 Analysis on SNR in Downstream

The signal light (at wavelength λ_1), the pilot light (at wavelength λ_1) and the LO light (at wavelength λ_2) all go through EDFAs before reaching the front end of coherent receiver. The receiver noise is dominated by the EDFA ASE. Therefore in the following noise analysis the electric noise including the shot noise and the thermal noise will be neglected.

Fig.7 indicates that the electric field (E_s) of signal light and the electric field (E_p) of pilot light have the same wavelength, but orthogonal polarization directions. The LO electric field (E_L) has a difference wavelength with frequency deviation δf . Each light has an ASE noise background.

In the heterodyne receiver, photodiode 1 carries out the square operation as:

$$i_1(t)\propto$$
$$\frac{1}{2}R\left|\begin{array}{l}\sqrt{\alpha}(E_s\sum_k\beta A_k e^{-\mathrm{j}[2\pi kf_s t+\theta_k]}e^{\mathrm{j}[\omega_{c1}t+\phi_c(t)]}+n_s(t)e^{\mathrm{j}[\omega_{c1}t+\phi_c(t)]})\\+\sqrt{1-\alpha}(E_p e^{\mathrm{j}[\omega_{c1}t+\phi_c(t)]}+n_p(t)e^{\mathrm{j}[\omega_{c1}t+\phi_c(t)]})\\+\frac{1}{\sqrt{2}}(E_L e^{\mathrm{j}[\omega_{c2}(t)+\phi_c(t)]}+n_L(t)e^{\mathrm{j}[\omega_{c2}t+\phi_c(t)]})\}\end{array}\right|^2$$

where $\dot{E}_s(t)=E_s\sum_k\beta A_k e^{-\mathrm{j}[2\pi kf_s t+\theta_k]}$, E_p, E_L are the electric field envelope of modulated signal light, pilot light, and LO light; The angular frequency ω_{c1} corresponds to wavelength λ_1; The angular frequency ω_{c2} corresponds to wavelength λ_2; $\phi_c(t)$ is the random phase of the optical comb.

Optical mixing results in many products falling to the baseband and being filter out, which include the self-beat terms $\left|\dot{E}_s(t)\right|^2$, $E_p{}^2$, $E_L{}^2$, $\left|n_s(t)\right|^2$, $\left|n_p(t)\right|^2$, $\left|n_L(t)\right|^2$ and the homodyne terms $\dot{E}_s(t)\times n_s(t)$, $E_p(t)\times n_p(t)$, $E_L(t)\times n_L(t)$, $\dot{E}_s(t)\times n_p(t)$, $E_p(t)\times n_s(t)$. The resulted heterodyne terms are the signal beat $\dot{E}_s(t)\times E_L$, $E_p\times E_L$ and the signal–ASE beat noise $\dot{E}_s(t)\times n_L(t)$, $E_L\times n_s(t)$, $E_L\times n_p(t)$, $E_p(t)\times n_L(t)$, which are located in IF band and picked out by a 12.5GHz band-pass filter. The ASE-ASE beat terms $n_s(t)\times n_p(t)$, $n_s(t)\times n_L(t)$, $n_p(t)\times n_L(t)$ are also falling in IF band, but omitted because they are relatively small.

The IF signal components in $i_1(t)$ are

$$R[\sqrt{\frac{\alpha}{2}}E_s\sum_k \beta A_k e^{-\mathrm{j}(2\pi k f_s t+\theta_k)}E_L + \sqrt{\frac{1-\alpha}{2}}E_L E_p]2\cos(2\pi\times\delta f\times t)$$

The IF signal-ASE beat noise components are

$$R\{\sqrt{\frac{\alpha}{2}}[E_s\sum_k \beta A_k e^{-\mathrm{j}(2\pi k f_s t+\theta_k)}n_L(t)+E_L n_s(t)]+ \sqrt{\frac{1-\alpha}{2}}[E_L n_p(t)+E_p(t)n_L(t)]\}2\cos(2\pi\times\delta f\times t)$$

The same operation taken in photodiode 3 produces $i_3(t)=-i_1(t)$, so that $i_1(t)-i_3(t)$ from the first balanced photodiode pair is

$$\begin{aligned}&2R\{\sqrt{\frac{\alpha}{2}}E_s\sum_k \beta A_k e^{-\mathrm{j}(2\pi k f_s t+\theta_k)}E_L + \sqrt{\frac{1-\alpha}{2}}E_L E_p\}2\cos(2\pi\times\delta f\times t)\\ &+2R\{\sqrt{\frac{\alpha}{2}}[E_s\sum_k \beta A_k e^{-\mathrm{j}(2\pi k f_s t+\theta_k)}n_L(t)+E_L n_s(t)] + \sqrt{\frac{1-\alpha}{2}}[E_L n_p(t)+E_p n_L(t)]\}2\cos(2\pi\times\delta f\times t)\end{aligned}$$

The photo-current $i_2(t)-i_4(t)$ output from the second balanced photodiode pair is

$$\begin{aligned}&2R\{\sqrt{\frac{\alpha}{2}}E_s\sum_k \beta A_k e^{-\mathrm{j}(2\pi k f_s t+\theta_k)}E_L + \sqrt{\frac{1-\alpha}{2}}E_L E_p\}2\sin(2\pi\times\delta f\times t)\\ &+2R\{\sqrt{\frac{\alpha}{2}}[E_s\sum_k \beta A_k e^{-\mathrm{j}(2\pi k f_s t+\theta_k)}n_L(t)+E_L n_s(t)] + \sqrt{\frac{1-\alpha}{2}}[E_L n_p(t)+E_p n_L(t)]\}2\sin(2\pi\times\delta f\times t)\end{aligned}$$

In down-conversion, the 12.5 GHz carrier is first extracted and amplified, then mixed with the IF signal and IF signal-ASE beat noise. After filtering out the DC and double frequency components, the output baseband signal and noise are

$$\{4R\sqrt{\frac{\alpha}{2}}\sum_k \beta A_k e^{-\mathrm{j}(2\pi k f_s t+\theta_k)}E_s E_L + 4R\sqrt{\frac{\alpha}{2}}E_L n_s(t) +4R\sqrt{\frac{1-\alpha}{2}}[E_L n_p(t)+E_p n_L(t)]\}4R\sqrt{\frac{1-\alpha}{2}}E_L E_p\sqrt{G}$$

where G is the gain of IF amplifier.

The average baseband signal power in the n-th sub-band is

$$S=1024R^4 G\alpha(1-\alpha)\beta^2\sigma_n^2 P_s P_p P_L{}^2 \tag{24}$$

The power of baseband signal-ASE beat noise in a sub-band is

$$\begin{aligned}N_{S-ASE}=&256R^4 G\{\alpha(1-\alpha)P_p P_L{}^2 N_s(\Delta f)\\ &+(1-\alpha)^2[P_p P_L{}^2 N_p(\Delta f)+P_L P_p{}^2 N_L(\Delta\nu)]\frac{1}{N}\}\end{aligned} \tag{25}$$

where $\Delta\nu_L$ is the bandwidth of LO optical filter; $\Delta f=Nf_s$ is the receiver bandwidth. By setting $\xi=\Delta\nu_L/\Delta f$, (25) becomes

$$\begin{aligned}N_{S-ASE}=&256R^4 G\{\alpha(1-\alpha)P_p P_L{}^2 N_s\\ &+(1-\alpha)^2[P_p P_L{}^2 N_p+P_L P_p{}^2 N_L\xi]\}f_s\end{aligned} \tag{26}$$

The signal to noise ratio is

$$\mathrm{SNR}_n=\frac{S}{N_{S,ASE}} =\frac{4\alpha\beta^2\sigma_n{}^2 P_s P_L}{\{\alpha P_L N_s+(1-\alpha)[P_L N_p+P_p N_L\xi]\}f_s} \tag{27}$$

where $\sigma_n{}^2=\mathrm{E}\{A_n^2\}/2$ is the mean square amplitude of OFDM signal in single sub-channel. Because $\beta^2\sigma_n^2\ll 1$, the subcarrier-LO ASE beat noise power has been omitted in (26).

N_s, N_p and N_L are ASE power spectrum of signal light, pilot light and LO light. Because the signal light and pilot light go through the same EDFA, i.e. $N_s=N_p$, The SNR can be simplified to

$$\mathrm{SNR}=\frac{4\alpha P_s P_L\beta^2\sigma_n^2}{[P_L N_p+(1-\alpha)P_p N_L\xi]f_s} \tag{28}$$

6 Optimization of EVM and BER

On the receiver side of the downstream OFDM transmission system, the non-linear distortion products of OFDM signal caused by the IQ modulator behave as an interfering noise to sub-carrier channel which superimposes on the white noise floor determined by the signal-ASE beat noise and degrades the average bit error rate (BER) of OFDM demodulator. Therefore, the conventional formula of BER for M-QAM OFDM scheme should be expanded to include the effect of interfering noise as

$$P_M \approx \frac{2}{\log_2 M}(1-\frac{1}{\sqrt{M}})\times \mathrm{erfc}\left[\sqrt{\frac{3}{2(M-1)}\times\frac{1}{\mathrm{EVM}^2}}\right] \quad (29)$$

where P_M is the bit error rate (BER); EVM is the error vector magnitude, which is determined jointly by SNR and CTB as

$$\mathrm{EVM}^2 = \frac{1}{\mathrm{SNR}_n} + \mathrm{CTB}_n \quad (30)$$

In the OFDM signal band, the white noise is normally flat over different sub-channels, but the composite triple beat power is dependent on the position of sub-channel within the band. Regularly in the center of OFDM signal band the composite triple beat power is highest (C_{3n} is maximum). Therefore when measuring the transmission performance in the worst case, one should consider the effect of composite triple beat in the central part of sub-channels.

Substituting (28) for SNR_n and (23) for CTB_n in (30) gives

$$\mathrm{EVM}^2 = \frac{N[P_L N_p + (1-\alpha)P_p N_L \xi] f_s}{\alpha P_s P_L \mu^2} + \frac{7C_{3n}}{576N^2}\mu^4 \quad (31)$$

where μ^2, the mean square optical modulation index, is proportional to the average power of driving OFDM signal:

$$\mu^2 = (\frac{\pi}{V_\pi})^2 \sigma_v^2, \quad \sigma_v^2 = N\sigma_n^2 \quad (32)$$

To minimize EVM^2 and BER, in addition to reducing the ASE spectrum and increasing the LO power as possible, the optimization of OFDM power driving to the IQ modulator is also important. Viewing (32), (33) finds that if the single sub-carrier power is higher, then SNR is higher, but CTB is even higher, therefore an optimal value of σ_n^2 exists which minimizes EVM. Let the derivative of EVM^2 with respect to μ^2 be zero, we find μ_{opt}^2 satisfying

$$\frac{7C_{3n}}{576N^2}(\mu_{\mathrm{opt}}^2)^2 = \frac{N[P_L N_p + (1-\alpha)P_p N_L \xi] f_s}{2\alpha P_s P_L \mu_{\mathrm{opt}}^2} \quad (33)$$

$$\mu_{\mathrm{opt}}^2 \approx N \times \sqrt[3]{\frac{[P_L N_p + (1-\alpha)P_p N_L \xi] f_s}{0.0243 \times \alpha P_s P_L C_{3n}}} \quad (34)$$

The corresponding $\mathrm{EVM}_{\min}^2$ is

$$\mathrm{EVM}_{\min}^2 = 3 \times \frac{7C_{3n}}{576N^2}(\mu_{\mathrm{opt}}^2)^2 \quad (35)$$

(33) means the optimal mean square optical modulation index making CTB to be a half of SNR^{-1}. (35) shows that the minimized EVM^2 is the triple times of CTB. To reduce $\mathrm{EVM}_{\min}^2$ lowering μ_{opt}^2 is necessary. This can be done by appropriately selecting the system optical power and the ASE parameter according to (34).

Computation is done for the following system parameters: signal wavelength $\lambda_1 =$ 1550.116nm; LO wavelength $\lambda_2 = 1550.216\mathrm{nm}$; OFDM bandwidth $B = Nf_s$=2GHz, N=64 (60 effective), f_s=31.25MHz; half-wave voltage $V_\pi = 2.8\mathrm{V}$, optical phase modulation index $\beta = \pi/(2V_\pi) = 0.561$ radian / V; polarization factor $\alpha = 0.5$. Received signal optical power P_s= −(10~30) dBm, Pilot optical power P_p= −5dBm, LO optical power P_L= −10~+5 dBm; Optical filter bandwidth ratio ξ=0.10~0.25 ; Photo-diode responsivity (including 90° hybrid loss) R= 0.08 A/W; C_{3n}=1305. ASE power spectrum N_p =-142.8 dBm/Hz and N_L =-142.3 dBm/Hz.

SNR is calculated versus P_L using (28) with the result shown in Fig.8. It is revealed that SNR increases with the LO power, but there is no benefit for very high LO power. Narrowing the optical filter bandwidth is useful.

The EVM^2 versus μ^2 is calculated using (31) and shown in Fig.9. The optimal mean square optical modulation index and the minimum EVM^2 are found to be 0.6 and 7% which are compliance with the results of (34) and (35).

The optimum OFDM power is found to be

$$P_{\mathrm{OFDM}} = \frac{\sigma_v^2}{R_L} = (\frac{V_\pi}{\pi})^2 \mu_{\mathrm{opt}}^2 \frac{1}{R_L} = 9.53\mathrm{mW} = 9.79\mathrm{dBm}$$

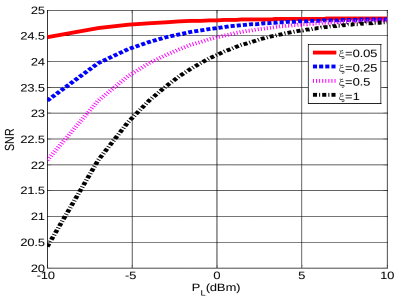

Fig.8 SNR vs P_L

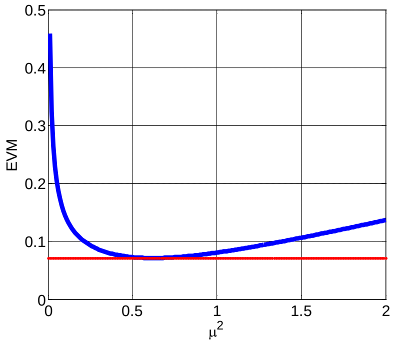

Fig.9 EVM^2 vs μ^2

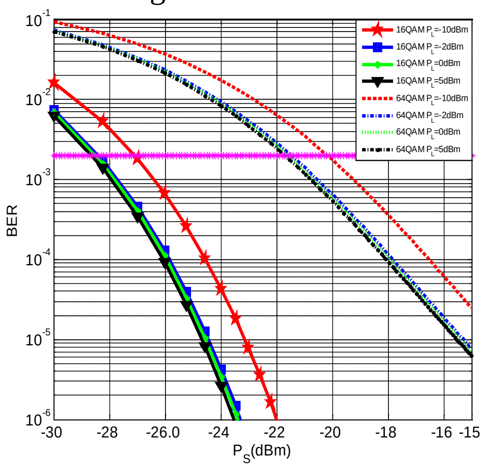

Fig.10 BER vs P_s

When the optimal μ^2 is used, the system BER versus received optical power P_S is drawn in Fig.10 for different LO power P_L. It is revealed that $P_L = -2$ dBm is enough for good BER performance. If 2×10^{-3} Pre-FEC BER is set to be the threshold to define receiver sensitivity, this OFDM-PON downstream link based on IQ modulation-heterodyne detection can have receiver sensitivity of –28.5 dBm.

7 Non-linear Optical Phase Noise Cancellation in Upstream

In the uplink ONU, the CW light at wavelength λ_2 injecting into RSOA is reflected, amplified and intensity-modulated by 1.6 GHz OFDM signal with 32 subcarriers. The bandwidth of RSOA is 1.6 GHz at 80 mA bias current and -2 dBm input optical power. The OFDM driving power is optimized by adjusting the non-linear distortion power in RSOA as a half of the ASE noise power received by OLT.

In receiver, the signal light carrying OFDM subcarriers beats with the LO light at the same wavelength, resulting in the following photo-currents of balanced PIN detectors as

$$i_i(t) = i_1(t) - i_3(t)$$
$$\propto 4RL\sqrt{P_S P_L}\sqrt{1+m\sum_{k=0}^{N\text{-}1} A_k \cos[2\pi k f_s (t-\frac{1}{2}\tau)+\phi_k]}$$
$$\times\cos[\theta_L(t)-\theta_L(t-\tau)-\delta\theta(t-\frac{1}{2}\tau)]$$
$$i_q(t) = i_2(t) - i_4(t)$$
$$\propto -4RL\sqrt{P_S P_L}\sqrt{1+m\sum_{k=0}^{N\text{-}1} A_k \cos[2\pi k f_s (t-\frac{1}{2}\tau)+\phi_k]}$$
$$\times\sin[\omega_c\tau+\theta_L(t)-\theta_L(t-\tau)-\delta\theta(t-\frac{1}{2}\tau)]$$

where m is the optical modulation index per unit current in RSOA; $\theta_L(t)$ is the optical phase of seeding light; $\delta\theta(t)$ is the optical phase shift induced by RSOA; τ is the time delay in the downstream and upstream round trip.

Because the OFDM signal is carried on the envelope of signal light, the optical phase is useless, therefore in the DSP a sum of squares operation on the above receiver outputs can be executed in the digital domain after ADC, so that the optical phase noise is cancelled out and the baseband OFDM signal is recovered as:

$$i_o^2(t) = i_i^2(t) + i_q^2(t)$$
$$= 16(RL)^2 P_S P_L[1+m\sum_{k=0}^{N\text{-}1} A_k \cos(2\pi k f_s t+\phi_k)]$$

In such a way the DSP algorithm is very simple, because the CPE frequency offset and carrier phase estimation is no longer necessary.

8 Experiment and Simulation

An experimental platform of OFDM-PON is set up according to Fig.1 including OLT, ODN and ONU. In OLT a 24λ optical comb is driven by a DFB laser source with 1 MHz line-width. An arbitrary waveform generator (Tek AWG 7122C) produces OFDM I and Q signals to modulate the signal light via a 40 Gb/s IQ modulator (Fujitsu FTM7962EP). In ODN, 20 km single mode fiber and Kylia DWDM multiplexers with wavelength interval 0.1nm are used. Wavelengths are checked with an optical spectrum analyser (AQ6370C). In ONU a coherent receiver is adopted to produce 4 outputs in push-pull manner which are observed with two spectrum analysers (N9010/30). The RF down converter is arranged as Fig.11 with a supper narrow (Q merit equal to 1000) band-pass filter centred at 12.5GHz to extract the IF carrier which is used to convert the sub-band OFDM signals down to baseband.

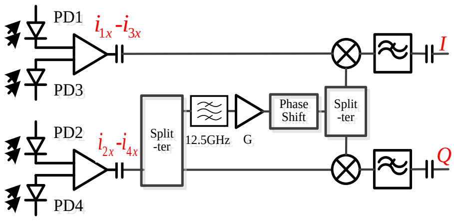

Fig.11 RF down-converter

The system input and output signals are shown in Fig,12. The input generated by AWG is a 64 sub-channel OFDM signal in 2 GHz band with a pre-enhanced slop of 6 dB/2GHz in order to ensure the flat output of coherent receiver. The dip in two central sub-channels is designed to check if the 3-rd order nonlinear distortion occurs after transmission.

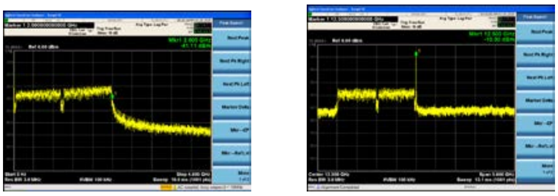

(a) Transmitted signal (b) Receiver output

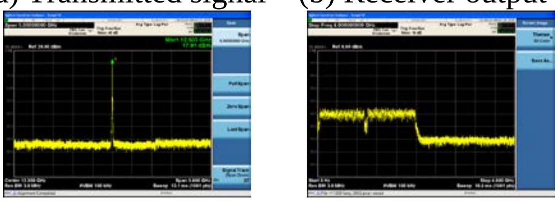

(c) Extracted IF carrier (d) Recovered signal

Fig.12 OFDM signal

The baseband OFDM signals (I & Q) output from the down-converters as in Fig.12 (d) are sampled to be series data by an oscilloscope (keysight 20 Gsa/s DSO-S 904A) with 10 bit ADC for the following DSP.

The DSP unit is an offline MATLAB software configured as Fig.13, in which the conventional CPE module is simplified to just contain a pilot tone-aided phase estimation algorithm to deal with the signal constellation dispersion and rotation caused by the residual optical phase noise and differential time delay.

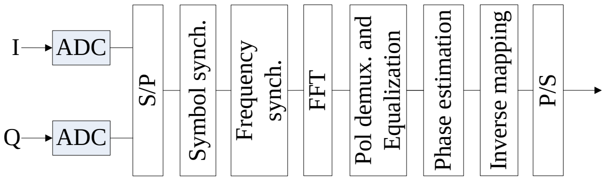

Fig. 13 DSP block

The measured BER versus P_s data points for 16QAM and P_L=–2dB are recorded as dark dots beside the theoretic curve in Fig.14, where the recovered constellations are also shown. There is roughly 1 dB difference between the theoretic and the practical result. This difference should

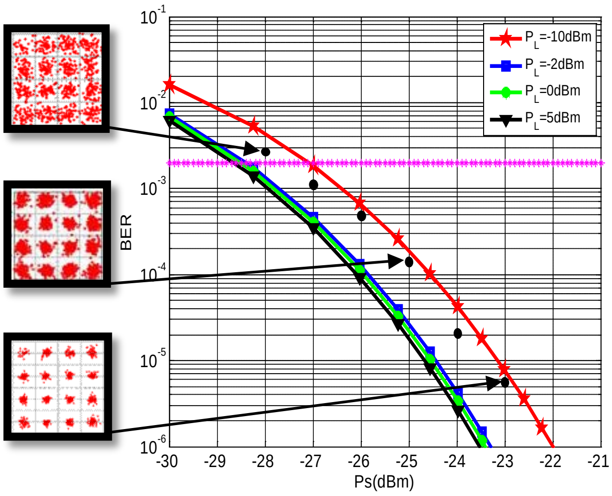

Fig.14 BER versus P_s

be the penalty caused by the link fiber in 20km

In upstream, the simulation was performed using VPI TransmissionMaker software added with a MATLAB algorithm for sum of squares operation. As results Fig.15 displays the spectra of intensity-modulated light and receiver output. The recovered 16QAM constellations are shown in Fig.16 and the BER curve with received optical power shown in Fig.17. It is found that the sensitivity of uplink receiver reaches –20 dBm at $2x10^{-3}$ BER, when the LO optical power is 0 dBm. The performance of uplink is obviously inferior to that of downlink. The improvement of receiver sensitivity is expected, if the LO power is higher.

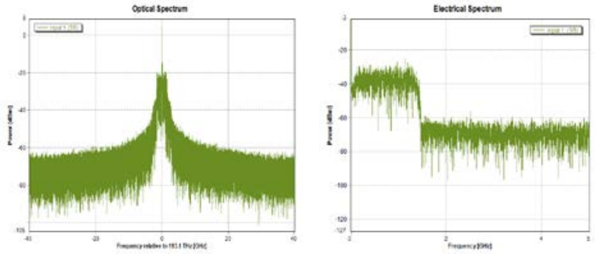

Fig. 15 Spectra of modulated light (left) and receiver output (right)

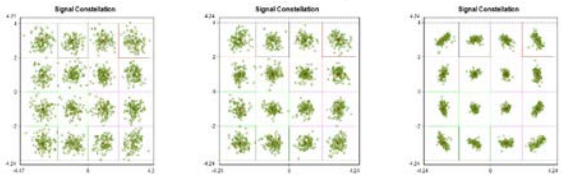

P_r=-22 dBm P_r=-18 dBm P_r=-12 dBm

Fig.16 Output signal constellation at P_L=0 dBm

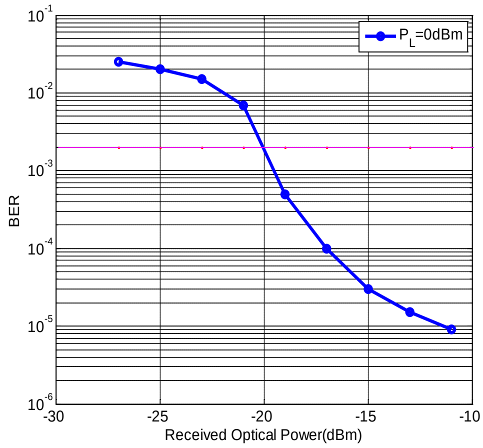

Fig.17 BER versus received optical power

9 Conclusion

A physical configuration of reflective 100/40 Gb/s OFDM-PON is proposed which works in coherent detection schemes to improve the link power budget. For the downstream link, IQ modulation-heterodyne detection is adopted. It is proved that the non-linearity tolerance of IQ optical modulator is much looser than that of MZM intensity modulator. By sharing the seed light power to RSOA, heterodyne detection can be carried out without an individual LO laser. By polarized pilot light multiplexing the optical phase noise in the heterodyne receiver output can be cancelled out in the RF down-conversion process if the delay difference between signal and pilot paths is eliminated. For the upstream link, the principle of non-linear optical phase noise is also discovered. These techniques may reduce system cost and DSP complexity and make the coherent detection in OFDM-PON reasonable. A system performance analytic model is given for EVM and BER optimization. As a result the receiver sensitivity of –(27~28.5) dBm is feasible for 16QAM format downlink which is much better than that of conventional intensity modulation-direct detection system. Further study is needed to improve the uplink.

Acknowledgement: This research has been supported by programs of National Natural Science Foundation of China (No. 61132004, 61275073，61420106011).

References

[1] Satoshi Shinada, Yukiyoshi Kamio, and Naoy, 16-QAM optical packet switching and real-time self-homodyne detection using polarization multiplexed pilot-carrier, *OPTICS EXPRESS*, Vol. 20, No. 26 , 2012, pp. B535-B542.

[2] Ruben S. Luís, et al., Self-Homodyne Detection of Polarization-Multiplexed Pilot Tone Signals Using a Polarization Diversity Coherent Receiver, *ECOC* 2013.

[3] Ruben S. Luís, et al., Self-Homodyne Coherent OFDM Packet Transmission without Carrier Frequency or Common Phase Error Estimation, *IEEE 4th International Conference on Photonics (ICP)*, 2013, pp. 123-125.

[4] S. Straullu, F. Forghieri, V. Ferrero, and R. Gaudino, Optimization of self-coherent reflective PON to achieve a new record 42 dB ODN power budget after 100 km at 1.25 Gbps, *OPTICS EXPRESS*, Vol.20, No. 28, 2012, pp. 29590-29598.

[5] Xiang Chen, et al., Tong Shao and Jianping Yao, Digital Phase Noise Cancellation for a Coherent-Detection Microwave Photonic Link，*IEEE Photonics Technology Letters*, Vol. 26, No. 8, April 15, 2014, pp.805-808.

[6] O. Shimbo, *Transmission Analysis in Communication Systems*, vol. I. Maryland: Computer Science Press, 1988.

[7] Rujian Lin, Analysis of OFDM Signal Distortion in Optical Fiber Links, *Asia Communications and Photonics*, 2011, Proceedings of SPIE-OSA-IEEE/Vol. 8309 83091C-1-14.